



# Deep-sea benthic megafaunal habitat suitability modelling: A global-scale maximum entropy model for xenophyophores



Oliver S. Ashford<sup>a,\*</sup>, Andrew J. Davies<sup>b</sup>, Daniel O.B. Jones<sup>a</sup>

<sup>a</sup> National Oceanography Centre, European Way, Southampton SO14 3ZH, UK

<sup>b</sup> School of Ocean Sciences, Bangor University, Menai Bridge, LL59 5AB, UK

## ARTICLE INFO

### Article history:

Received 18 March 2014

Received in revised form

15 July 2014

Accepted 20 July 2014

Available online 7 August 2014

### Keywords:

Maxent

Species distribution modelling

Xenophyophorea

*Syringammina fragilissima*

*Stannophyllum zonarium*

## ABSTRACT

Xenophyophores are a group of exclusively deep-sea agglutinating rhizarian protozoans, at least some of which are foraminifera. They are an important constituent of the deep-sea megafauna that are sometimes found in sufficient abundance to act as a significant source of habitat structure for meiofaunal and macrofaunal organisms. This study utilised maximum entropy modelling (Maxent) and a high-resolution environmental database to explore the environmental factors controlling the presence of Xenophyophorea and two frequently sampled xenophyophore species that are taxonomically stable: *Syringammina fragilissima* and *Stannophyllum zonarium*. These factors were also used to predict the global distribution of each taxon. Areas of high habitat suitability for xenophyophores were highlighted throughout the world's oceans, including in a large number of areas yet to be suitably sampled, but the Northeast and Southeast Atlantic Ocean, Gulf of Mexico and Caribbean Sea, the Red Sea and deep-water regions of the Malay Archipelago represented particular hotspots. The two species investigated showed more specific habitat requirements when compared to the model encompassing all xenophyophore records, perhaps in part due to the smaller number and relatively more clustered nature of the presence records available for modelling at present. The environmental variables depth, oxygen parameters, nitrate concentration, carbon-chemistry parameters and temperature were of greatest importance in determining xenophyophore distributions, but, somewhat surprisingly, hydrodynamic parameters were consistently shown to have low importance, possibly due to the paucity of well-resolved global hydrodynamic datasets. The results of this study (and others of a similar type) have the potential to guide further sample collection, environmental policy, and spatial planning of marine protected areas and industrial activities that impact the seafloor, particularly those that overlap with aggregations of these conspicuously large single-celled eukaryotes.

© 2014 Elsevier Ltd. All rights reserved.

## 1. Introduction

Xenophyophores represent some of the most remarkable megafauna in the deep sea. These giant rhizarian protozoans build agglutinated tests that, in some cases, reach diameters of over 20 cm (Tendal, 1972; Levin and Thomas, 1988; Gooday et al. 2011), and were first described in the late 19th century. Initially they were interpreted as a type of primitive foraminifera (Brady, 1883) or alternatively as a group of horny sponges living in symbiosis with hydroids (Haeckel, 1889). It was not until the early 20th century that xenophyophores were recognised and named as a well defined group at a high taxonomic level within rhizopod protozoans (Schulze, 1904, 1907; Tendal, 1972; Pawlowski et al. 2003). Even

with this taxonomic recognition, xenophyophores lingered in relative obscurity for much of the 20th century, and only after the publication of a landmark monograph in 1972 (Tendal, 1972) did the group become widely known amongst marine biologists in general (Gooday et al., 1993; Riemann et al., 1993; Pawlowski et al., 2003; Hughes and Gooday, 2004; Gooday et al., 2011).

Xenophyophores are a large, conspicuous component of the benthic megafauna found in all major ocean basins (Tendal, 1972; Levin, 1991; Levin and Gooday, 1992; Tendal, 1996) and can be enumerated in deep-water photographs (Kamenskaya et al., 2013) due to their often visually distinctive agglutinated tests. These tests enclose a branching system of organic tubes containing the cell body (the granellare system) together with often voluminous masses and strings of waste material (stercomata) enclosed within an organic membrane (Tendal, 1972; Gooday et al., 2011). However, observations of living specimens are limited, and so many aspects of xenophyophore biology, reproduction and life cycle remain obscure (Pawlowski et al., 2003).

\* Corresponding author. Present address: Department of Zoology, University of Oxford, Tinbergen Building, South Parks Road, Oxford OX1 3PS, UK.  
Tel.: +44 7763 018136.

E-mail address: [oliver.ashford@zoo.ox.ac.uk](mailto:oliver.ashford@zoo.ox.ac.uk) (O.S. Ashford).

Two major xenophyophore lineages are recognised based on morphological criteria: the Psamminida (4 families, 14 genera and over 50 described species), most of which have rigid tests, and the Stannomida (1 family, 2 genera and ~17 described species), whose tests are ramified by proteinaceous fibres (linellae) and are generally more flaccid (Tendal, 1972; Tendal, 1996; Gooday and Tendal, 2002; Bisby et al. 2010). Opinions about the phylogenetic position of xenophyophores have developed over time. Following initial attempts at classifying xenophyophores (Brady, 1883; Haeckel, 1889) (see above), Schulze (1907) concluded that they represent a distinct group of rhizopod protozoans, an opinion followed by many later workers (Tendal, 1972; Gooday and Tendal, 2002). Recently, however, phylogenetic analysis of small sub-unit ribosomal RNA sequences from *Syringammina corbicula* Richardson, 2001, *Aschemonella ramuliformis* Brady, 1884, *Shinkaiya lindsayi* Lecroq et al., 2009 and *Reticulammina cerebiformis* Gooday et al., 2011 (Pawlowski et al., 2003; Lecroq et al., 2009; Gooday et al., 2011) support Brady's (1883) conclusions that xenophyophores are foraminiferans. However, no sequence data yet exists for stannomids, and so it remains to be proven that all xenophyophores are foraminifera.

Confined to depths greater than about 500 m, xenophyophores reach peak densities where particle flux to the seafloor is enhanced, such as beneath productive surface waters, in canyons, on areas of raised topography (seamounts or ridges, for instance), or on continental slopes (Tendal, 1972; Tendal and Gooday, 1981; Levin et al., 1986; Levin and Thomas, 1988; Levin, 1994; Buhl-Mortensen et al., 2010; Gooday et al., 2011). Xenophyophores may live infaunally in soft mud, but most are epifaunal and live on soft sediment or attached to hard substrates (e.g. Tendal and Gooday, 1981; Gooday et al., 2011; Kamenskaya et al., 2013). They are likely to feed on a diet comprised mainly of detrital particles that are obtained via suspension feeding, surface-deposit feeding or by being trapped within the complex morphology of the test (Tendal, 1972; Lemche et al., 1976; Levin and Thomas, 1988; Gooday et al., 1993). It has further been suggested that xenophyophores are able to prey on small metazoans (Levin and Gooday, 1992; Smith et al., 2003), and may 'farm' microbes as secondary food sources (Tendal, 1979; Laureillard et al., 2004; Hori et al., 2013), although there is no direct evidence for either of these feeding modes (A. Gooday, personal communication).

Xenophyophores sometimes play a significant role in biological processes that occur at the sediment-water interface (Tendal, 1972; Levin and Thomas, 1988; Levin and Gooday, 1992) and large morphologically complex species of genera such as *Reticulammina* Tendal, 1972 and *Syringammina* Brady, 1883 can be considered as autogenic ecosystem engineers. For example, xenophyophore tests provide a focus for organic carbon deposition, serving as traps of organic-rich sedimenting particles and add physical heterogeneity to seafloor mineralisation processes (Levin and Thomas, 1988; Levin and Gooday, 1992). Xenophyophore tests further represent important habitat-forming structures on the seafloor, contributing significantly to deep-sea biological heterogeneity (Levin and Thomas, 1988; Levin, 1991; Levin and Gooday, 1992; Smith et al., 2003; Buhl-Mortensen et al., 2010; Hori et al. 2013). As a result, large complex tests appear to constitute faunal hotspots in the deep sea (Levin, 1991, 1994; Hughes and Gooday, 2004), with enhanced faunal densities and species richness (particularly of crustaceans, molluscs, echinoderms, foraminifera and bacteria) in their close vicinity (Levin et al., 1986; Hori et al., 2013).

Because of these characteristics, some xenophyophore species may represent an effective umbrella taxon. Knowledge of their distributions therefore has the potential to be used as a guide, in addition to further information on the distribution of vulnerable marine ecosystems, as to which regions could be designated as marine protected areas (MPAs). Certain areas with abundant

xenophyophores may be important for deep-sea biodiversity and so should be considered for protection from human practices that disturb the seafloor, like deep-sea trawling, oil and gas extraction and mining.

The great utility of global habitat suitability modelling is in the determination of the potential distributions of taxa that cannot be easily mapped using traditional methods. This is commonly the case in deep-water marine environments, which are difficult to sample due to barriers of cost and isolation. Species distribution models are informative in the context of general scientific investigations (e.g. in targeting regions for further research). In addition, where the investigated group is of conservation concern because of its vulnerability to anthropogenic disturbance and/or important in the functioning of ecosystems, these models can be instructive in directing the designation of protected areas (Davies and Guinotte, 2011; Yesson et al., 2012). Maximum entropy habitat suitability modelling method that produces a niche model by minimising the relative entropy between two probability densities; one estimated from the input presence data and the other from the environmental parameters of the landscape in question (Tittensor et al., 2010; Elith et al., 2011). Maxent has been shown to be one of the highest performing (i.e. most accurate) habitat suitability modelling techniques available (Elith et al., 2006; Ortega-Huerta and Peterson, 2008; Wisz et al., 2008). However, its accuracy can drop substantially if a suitable number and variety of presence records are not available to guide the model, and/or if the environmental data available are not reliable or do not fully encompass the range of environmental factors experienced by the focus taxon. There are known issues associated with species distribution models based on small numbers of presence records (Feely and Silman, 2011), including over-prediction, resulting in false positives (Anderson and Gonzalez, 2011), and false negatives. In terms of environmental variables, obtaining a high-resolution global dataset currently requires up-scaling from lower-resolution data, and this inevitably introduces some error, which grows as the difference between native and required resolution increases (Davies and Guinotte, 2011). On balance however, distribution modelling at a global scale remains an instructive and informative technique.

This manuscript uses predictive habitat modelling to assess the global probability of occurrence of xenophyophores as a whole taxon and to explore the potential global distribution of the two most commonly recorded xenophyophore species that are also considered taxonomically stable: *Syringammina fragilissima* Brady, 1883 and *Stannophyllum zonarium* Haeckel, 1889. Xenophyophore distributions are modelled using a 30'' environmental database, which allows for global modelling at relatively fine spatial scales.

## 2. Methods

### 2.1. Xenophyophore presence data

A total of 837 independent presence records representing 68 xenophyophore species was obtained from peer-reviewed journals, cruise reports, the Global Biodiversity Information Facility (GBIF) and Ocean Biogeographic Information System (OBIS) (Table 1, Table S1). Prior to analysis, this dataset was revised so that only a single record was retained within each 30'' cell since multiple presence localities within a single 30'' cell can cause habitat suitability values to be weighted in favour of the environmental conditions that exist in that cell (Davies and Guinotte, 2011). As a result, 569 presence records were retained for the distribution modelling of Xenophyophorea, 40 for *S. fragilissima*, and 31 for *S. zonarium* (Table 1).

**Table 1**

Number of geo-referenced records available per xenophyophore taxon. Only one record per 30'' cell was retained for Maxent analyses. Number of species for which geo-referenced records were available = 68.

Genus	Species	No. records	No. records retained in analysis	
<b>Aschemonella</b>	<i>carpathica</i>	5		
	<i>catenata</i>	4		
	<i>composita</i>	12		
	<i>grandis</i>	9		
	<i>ramuliformis</i>	85		
	<i>scabra</i>	80		
	Unknown	58		
<b>Cerelasma</b>	<i>gyrosphaera</i>	2		
	<i>lamellosa</i>	1		
	<i>massa</i>	7		
<b>Cerelpepma</b>	Unknown	1		
	<i>radiolarium</i>	4		
<b>Galatheaemmina</b>	<i>calcareo</i>	9		
	<i>discoveryi</i>	4		
	<i>erecta</i>	13		
	<i>lamina</i>	1		
	<i>microconcha</i>	3		
	<i>tetraedra</i>	4		
	Unknown	7		
<b>Holopsamma</b>	<i>argillaceum</i>	1		
	<i>cretaceum</i>	1		
<b>Homogamma</b>	<i>lamina</i>	13		
	<i>maculosa</i>	20		
	Unknown	3		
<b>Maudamma</b>	<i>arenaria</i>	1		
	<i>tenera</i>	2		
<b>Nazaremma</b>	<i>profunda</i>	1		
	Unknown	1		
<b>Psammetta</b>	<i>arenocentrum</i>	1		
	<i>erythrocytomorpha</i>	3		
	<i>globosa</i>	6		
	Unknown	4		
<b>Psamma</b>	<i>delicate</i>	6		
	<i>fusca</i>	1		
	<i>globigerina</i>	3		
	<i>nummulina</i>	4		
	<i>plakina</i>	1		
	<i>sabulosa</i>	3		
	<i>zonaria</i>	1		
	Unknown	12		
	<b>Psammopemma</b>	<i>calcareum</i>	1	
	<b>Reticulammina</b>	<i>antarctica</i>	1	
<i>cerebreformis</i>		10		
<i>cretacea</i>		1		
<i>labyrinthica</i>		34		
<i>lamellata</i>		3		
<i>maini</i>		1		
<i>novaezealandica</i>		3		
<i>plicata</i>		1		
Unknown		26		
<b>Semipsamma</b>		Unknown	2	
<b>Shinkaiya</b>	<i>lindsayi</i>	1		
<b>Spiculamma</b>	<i>delicata</i>	1		
<b>Stannarium</b>	<i>concretum</i>	1		
<b>Stannoma</b>	<i>alatum</i>	1		
	<i>coralloides</i>	5		
<b>Stannophyllum</b>	<i>dendroides</i>	11		
	Unknown	1		
	<i>alatum</i>	4		
	<i>annectens</i>	1		
	<i>concretum</i>	1		
	<i>flustraceum</i>	2		
	<i>fragilis</i>	1		
	<i>globigerinum</i>	19		
	<i>granularium</i>	11		
	<i>indistinctum</i>	3		
	<i>mollum</i>	9		
	<i>pertusum</i>	1		
	<i>radiolarium</i>	3		
<i>reticulatum</i>	2			
<i>setosum</i>	1			
<i>venosum</i>	1			

**Table 1 (continued)**

Genus	Species	No. records	No. records retained in analysis
<b>Syringamma</b>	<i>zonarium</i>	31	31
	Unknown	3	
	<i>corbicula</i>	4	
	<i>fragilissima</i>	49	40
	<i>minuta</i>	1	
	<i>reticulata</i>	2	
	<i>tasmanensis</i>	7	
<b>Unknown</b>	Unknown	10	
		170	
<b>Total</b>		837	569

Producing a robust species-level distribution model requires a sufficient number of presence records to represent the full observed niche of the species in question as well as confidence in the taxonomic stability and consistency of identification of the chosen species (i.e. that all available records represent a single species, rather than a suite of morphologically similar species). *A. ramuliformis* Brady, 1879, *Aschemonella scabra* Brady, 1879 and *Reticulammina labyrinthica* Tendal, 1972 fit this first requirement, with a large number of geo-referenced samples available relative to other xenophyophore species (Table 1). However, there is considerable doubt concerning the taxonomic status of these *Aschemonella* species, and they are probably morphotypes that encompass several similar species rather than representing discrete and consistently identified species (A. Gooday, personal communication). This concern also extends to *R. labyrinthica*, since it is unlikely that this name has been applied consistently in the literature (A. Gooday, personal communication). As a result, only two species remained for which numerically sufficient taxonomically reliable geo-referenced records were available: *S. fragilissima* and *S. zonarium*. Hence, only these species were subjected to distribution modelling.

## 2.2. Environmental data

In total, 25 environmental layers were produced for use in the Maxent (maximum entropy; Phillips et al., 2006) models (Table 2, and see Fig. S4 for a correlation matrix of these layers). These were chosen both for their ecological relevance and their availability at a global scale. They can be split into six broad categories: bathymetric variables (layers derived from a bathymetric grid), carbonate chemistry variables (measures of calcite saturation state), chemical variables (general chemical parameters including salinity, alkalinity and dissolved inorganic carbon amongst others), hydrodynamic variables (current flow), oxygen variables (combination of variables relating to oxygen availability and utilisation), and temperature variables (after Yesson et al., 2012). Productivity variables were not available owing to a rapid decline in data quality at latitudes greater than ~70°N and S. Since all environmental grids must be of the same latitudinal extent for use in Maxent, and about 22% of xenophyophore presence records were from over 70°N, the decision was made to abandon the use of productivity variables in order to maximise the number of presence records used in the models. However, apparent oxygen utilisation (AOU) was available as a variable, and can be considered a proxy for respiration, which in turn correlates with rates of particulate organic carbon (POC) reaching the benthos (Pfannkuche, 1993). AOU refers to the difference in dissolved oxygen concentration of a body of water and its equilibrium oxygen saturation concentration under the same physical and chemical parameters – relating to the use of oxygen due to organismal respiration (Garcia et al., 2006a).

**Table 2**  
Summary of geophysical and environmental variables used in this study. All variables are stored in an ArcGIS file geo-database. Superscript notes indicate particular analysis or treatment of data.

Variable group	Variable	Units	Reference
<b>Bathymetric variables<sup>1</sup></b>			
	Aspect	Deg	Jenness (2012)
	Aspect - Eastness <sup>2,3</sup>	Deg	Wilson et al. (2007)
	Aspect - Northness <sup>2,4</sup>	Deg	Wilson et al. (2007)
	Curvature - Plan <sup>5,7</sup>		Jenness (2012)
	Curvature - Profile <sup>5,6</sup>		Jenness (2012)
	Curvature - Tangential <sup>5,8</sup>		Jenness (2012)
	Depth	m	Becker et al. (2009)
	Roughness <sup>9</sup>		Wilson et al. (2007)
	Rugosity <sup>5</sup>		Jenness (2012)
	Slope <sup>5</sup>	Deg	Jenness (2012)
	Terrain Ruggedness Index <sup>9</sup>		Wilson et al. (2007)
	Topographic Position Index <sup>9</sup>		Wilson et al. (2007)
<b>Carbonate chemistry variables</b>			
	Calcite saturation state <sup>10,11</sup>	$\Omega_{\text{CALC}}$	Steinacher et al. (2009)
<b>Chemical variables</b>			
	Alkalinity <sup>10</sup>	$\mu\text{mol l}^{-1}$	Steinacher et al. (2009)
	Dissolved inorganic carbon <sup>10</sup>	$\mu\text{mol l}^{-1}$	Steinacher et al. (2009)
	Nitrate <sup>10</sup>	$\mu\text{mol l}^{-1}$	Garcia et al. (2006b)
	Phosphate <sup>10</sup>	$\mu\text{mol l}^{-1}$	Garcia et al. (2006b)
	Salinity <sup>10</sup>	pss	Boyer et al. (2005)
	Silicate <sup>10</sup>	$\mu\text{mol l}^{-1}$	Garcia et al. (2006b)
<b>Hydrodynamic variables</b>			
	Regional flow <sup>12</sup>	$\text{m s}^{-1}$	Carton et al. (2005)
	Vertical flow <sup>12</sup>	$\text{m s}^{-1}$	Carton et al. (2005)
<b>Oxygen variables</b>			
	Apparent oxygen utilisation <sup>10</sup>	$\text{mol m}^{-3}$	Garcia et al. (2006a)
	Dissolved oxygen concentration <sup>10</sup>	$\text{ml l}^{-1}$	Garcia et al. (2006a)
	Per cent oxygen saturation <sup>10</sup>	$\% \text{O}_2$	Garcia et al. (2006a)
<b>Temperature variables</b>			
	Temperature <sup>10</sup>	$^{\circ}\text{C}$	Boyer et al. (2005)

<sup>1</sup> Derived from SRTM30 bathymetry.

<sup>2</sup> Calculated in ArcGIS 10.

<sup>3</sup> Modified calculation from Wilson et al. (2007) using  $\text{Sin}(\text{Aspect } \pi)/180$ , to produce 1 = east and -1 = west orientation.

<sup>4</sup> Modified calculation from Wilson et al. (2007) using  $\text{Cos}(\text{Aspect } \pi)/180$ , to produce 1 = north and -1 = south orientation.

<sup>5</sup> Calculated using the 4 cell method in Jenness (2012).

<sup>6</sup> Longitudinal curvature in Jenness (2012) and defined as "Longitudinal curvatures are set to positive when the curvature is concave (i.e. when water would decelerate as it flows over this point). Negative values indicate convex curvature where stream flow would accelerate." Zero indicates an undefined value.

<sup>7</sup> Defined in Jenness (2012) as "Plan curvatures are set to positive when the curvature is convex (i.e. when water would diverge as it flows over this point). Negative values indicate concave curvature where stream flow would converge." Zero indicates an undefined value.

<sup>8</sup> Defined in Jenness (2012) as "Tangential curvatures are set to positive when the curvature is convex (i.e. when water would diverge as it flows over this point). Negative values indicate concave curvature where stream flow would converge." Zero indicates an undefined value.

<sup>9</sup> Calculated using GDAL DEM Tool. Values at zero indicate flat areas, higher values indicate rough and variable terrain.

<sup>10</sup> Variable creation process followed the Davies and Guinotte (2011) upscaling approach.

<sup>11</sup> Created using SRES1B scenario data from the years 2000–2010.

<sup>12</sup> SODA data extracted from version 2.0.4, monthly means for the years 1990–2007.

Terrain attributes were extracted from bathymetric data (SRTM30 – a topographical layer produced from a combination of data from the U.S. 'Shuttle Radar Topography Mission' and the U.S. Geological Survey's 'Global 30" Elevation Data Set') following techniques and algorithms described in Wilson et al. (2007). Individual approaches are detailed in footnotes within Table 2; a brief description of each variable is given here. Topographic

position index (TPI) is an approach to determine topographical features based on their relative position within a neighbourhood, and can be calculated over fine or broad scales to capture smaller or larger terrain features respectively. This calculation has been developed into a GDAL tool (Geospatial Data Abstraction Library) and the approach is described in Wilson et al. (2007). Slope was calculated using DEM Tools for ArcGIS developed by Jenness (2012), in particular the 4-cell method of calculating slope, which is accepted as the most accurate approach (Jones, 1998). Here, slope is defined as the gradient in the direction of the maximum slope. Curvature attempts to describe general terrain features and may provide an indication of how water interacts with the terrain. Plan and tangential curvature describe how water converges or diverges as it flows over relief, whilst profile curvature describes how water accelerates or decelerates as it flows over relief (Jenness, 2012). Aspect is defined as the direction of maximum slope and was converted to continuous radians following Wilson et al. (2007). Rugosity, terrain ruggedness index and roughness all describe the variability of the relief of the seafloor (Wilson et al., 2007). Rugosity is defined as the ratio of the surface area to the planar area across a neighbourhood of a central pixel (Jenness, 2012) while terrain ruggedness index is defined as the mean difference between a central pixel and its surrounding cells and roughness as the largest inter-cell difference of a central pixel and its surrounding cell (Wilson et al., 2007). Roughness is calculated as the difference in value between the minimum and maximum bathymetry within a neighbourhood (Wilson et al., 2007).

All other variables were created using the up-scaling approach presented within Davies and Guinotte (2011). All data were available in a gridded form partitioned into standardised depth bins ('z-layers') with a depth range of ~0–5500 m. These z-layers facilitated the determination of approximate benthic habitat conditions (of greatest interest owing to the benthic nature of xenophophores) on a global scale. This was achieved by the projection of each z-layer to its corresponding area of seafloor using the up-scaling approach (Davies and Guinotte, 2011). This process involved three steps. (1) Each z-layer was initially interpolated using inverse-distance weighting to a slightly higher spatial resolution (usually  $0.1^{\circ}$ ) in order to minimise potential gaps that could appear between adjacent z-layers due to non-overlap following projection on to the bathymetric layer. (2) These layers were re-sampled to match SRTM30 (Becker et al., 2009) resolution (the highest resolution global bathymetric dataset available) and so preserve as high a spatial resolution as possible. (3) Each re-sampled z-layer was draped over the SRTM30 bathymetric layer to provide an indication of conditions near the seabed. Due to the limitations of the global datasets currently available, it had to be assumed that conditions below the deepest z-layer available were stable to the seabed. However, this approach has been demonstrated to work well over global and regional scales (Davies and Guinotte, 2011; Guinotte and Davies, 2012).

Since the incorporation of too many variables into a habitat suitability model can cause over-fitting of the model (Beaumont et al., 2005), a small subset of the available environmental layers was selected for use in the final analyses. Owing to the co-variant nature of many of the layers in each of the six variable categories (Fig. S4), a single variable from each category was selected to represent the influence of that category (following the method of Yesson et al., 2012). Variable selection for each category was based on the predictive power of models based on single environmental layers. This was measured using the Test AUC statistic (area under the receiver operating characteristic – ROC – curve; Fielding and Bell, 1997). The AUC statistic can be defined as the probability that a presence site is ranked above a random background site. Values vary from 0 (model performance worse than random) to 0.5 (model performance indistinguishable from random) to 1 (model



is maximally predictive) (Fielding and Bell, 1997). Test AUC is quoted since it is more reliable than training AUC scores (Warren and Seifert, 2011). Thus the single variable that produced the greatest test AUC value in isolation for each biological category was selected to represent that category in the final analyses, and hence the final analyses utilised six environmental layers (Tables 3 and 4).

### 2.3. Maximum entropy predictions

Maxent (Phillips et al., 2006) version 3.3.3 k was used to perform the global distribution prediction analyses. The following default model parameters were used: convergence threshold of  $10^{-5}$ , regularisation parameter of 1 and a maximum iterations value of 500, with 10,000 points randomly selected as background data to construct the model and each model run setting aside 30% of presence records for model evaluation. These settings have been shown to produce reliable results (Phillips and Dudik, 2008; Davies and Guinotte, 2011; Yesson et al., 2012). Higher regularisation parameter values were trialled for the more taxonomically inclusive model of Xenophyophorea to produce smoother response curves (Fig. 2). However, this resulted in the production of over-generalised models, lower test AUC, increased differences between training and test AUC, and a less discriminatory model output.

Model performance was evaluated by considering entropy, test AUC, test gain, and test omission scores (see Phillips et al., 2006). The importance of each environmental variable was assessed using a jack-knifing procedure by comparing the gain achieved by variables in isolation (jack-knife of regularised training gain). Response curves were produced to visualise how xenophyophore habitat suitability varied with each environmental factor analysed.

**Table 4**

Model evaluation statistics for global Maxent habitat suitability models of xenophyophore taxa based on multiple variables. The three most important variables for each taxon (jack-knife of regularised training gain) are highlighted in bold and underlined.

Statistic	Xenophyophorea	<i>Syringammina fragilissima</i>	<i>Stannophyllum zonarium</i>
<b>Model evaluation</b>			
Test AUC	0.836	0.997	0.941
Test gain	0.841	4.580	1.768
Entropy	8.632	4.512	7.551
<b>Threshold</b>			
Logistic value	0.379	0.100	0.276
Test omission (%)	0.200	0.000	0.000
Fractional predicted area	0.244	0.010	0.124
Probability	$4.83 \times 10^{-64}$	$7.59 \times 10^{-25}$	$6.70 \times 10^{-9}$
<b>Regularised training gain in isolation</b>			
Depth	0.228	<b><u>3.153</u></b>	0.109
Calcite saturation state	0.114	<b><u>2.115</u></b>	0.172
Dissolved inorganic carbon	–	1.848	–
Nitrate	<b><u>0.331</u></b>	–	<b><u>1.254</u></b>
Regional flow	0.004	0.608	0.016
Apparent oxygen utilisation	–	1.618	<b><u>1.450<sup>a,b</sup></u></b>
Per cent oxygen saturation	<b><u>0.286</u></b>	–	–
Temperature	<b><u>0.339<sup>a,b</sup></u></b>	<b><u>3.241<sup>a,b</sup></u></b>	<b><u>0.441</u></b>

<sup>a</sup> Indicates the variable that reduced the training gain most when omitted and therefore contained the most useful information that was not present in other variables.

<sup>b</sup> Indicates the variable with the highest training gain when used in isolation and which thus had the most useful information by itself. Thresholds are based on the maximum sensitivity plus specificity of the test dataset.

**Table 3**

Test AUC values for global Maxent habitat suitability models of xenophyophore taxa based on single variables. The highest AUC scores in each variable group are highlighted in bold and underlined for each taxon.

Variable group	Variable	Xenophyophorea	<i>Syringammina fragilissima</i>	<i>Stannophyllum zonarium</i>
<b>Bathymetric variables</b>				
	Aspect	0.535	0.672	0.615
	Eastness of aspect	0.514	0.509	0.507
	Northness of aspect	0.518	0.614	0.529
	Plan curvature	0.562	0.500	0.500
	Profile curvature	0.577	0.500	0.500
	Tangential curvature	0.560	0.500	0.500
	Depth	<b><u>0.686</u></b>	<b><u>0.987</u></b>	<b><u>0.696</u></b>
	Roughness	0.571	0.548	0.666
	Rugosity	0.544	0.583	0.688
	Terrain ruggedness index	0.561	0.574	0.659
	Topographic position index	0.598	0.393	0.408
	Slope	0.554	0.577	0.673
<b>Carbonate chemistry variables</b>				
	Calcite saturation state	<b><u>0.654</u></b>	<b><u>0.957</u></b>	<b><u>0.784</u></b>
<b>Chemical variables</b>				
	Alkalinity	0.669	0.961	0.808
	Dissolved inorganic carbon	0.689	<b><u>0.977</u></b>	0.840
	Nitrate	<b><u>0.728</u></b>	0.903	<b><u>0.913</u></b>
	Phosphate	0.703	0.935	0.891
	Salinity	0.714	0.834	0.318
	Silicate	0.717	0.931	0.908
<b>Hydrodynamic variables</b>				
	Regional flow	<b><u>0.500</u></b>	<b><u>0.810</u></b>	<b><u>0.633</u></b>
	Vertical flow	0.491	0.500	0.500
<b>Oxygen variables</b>				
	Apparent oxygen utilisation	0.733	<b><u>0.910</u></b>	<b><u>0.907</u></b>
	Dissolved oxygen concentration	0.725	0.873	0.895
	Per cent oxygen saturation	<b><u>0.747</u></b>	0.891	0.897
<b>Temperature variables</b>				
	Temperature	<b><u>0.720</u></b>	<b><u>0.986</u></b>	<b><u>0.776</u></b>

### 3. Results

#### 3.1. Sample locations

Xenophyophore sampling to date is patchily distributed throughout the world's oceans (Fig. 1). Areas where the highest numbers of xenophyophores have been collected include the North Atlantic (the Porcupine Abyssal Plain, Rockall Bank, Monaco Basin, Cape Verde Plateau and along the Mid-Atlantic Ridge), the Gulf of Mexico, the South Atlantic (especially around the Rio Grande Rise and Mid-Atlantic, Atlantic-Indian and Walvis Ridges) and Atlantic portion of the Southern Ocean, the Arctic Ocean (Baffin Basin, Barents Sea, Nansen Basin, Amundsen Basin and Makarov Basin in particular), parts of the Indian Ocean (Somali Basin and off the coast of South Africa in particular) the South China Sea, the Northwest Pacific Basin, the Peru Basin, and around New Zealand. In contrast, xenophyophores have been only sparsely collected from the majority of the Indian and Southern Oceans, the western Arctic Ocean, and the South Pacific Ocean.

The global distribution of xenophyophore samples (Fig. 1) cannot be directly interpreted in terms of overall sampling effort, but the patterns described above suggest that deep-water investigations are concentrated close to nations with more established sampling programmes, as well as hinting of potential bias against more remote locations (the Southern Ocean, for instance).

#### 3.2. Variable selection

Test AUC scores for the models based on a single variable varied greatly – from a minimum value of 0.393 (topographic position index, *S. fragilissima*) to a maximum of 0.987 (depth, *S. fragilissima*) (Table 3). Considering the six variable groupings (Table 2), depth performed best of all bathymetric variables across the taxa, whilst the curvature variables and topographic position index consistently produced some of the lowest AUC scores. Calcite saturation state returned high AUC scores for all taxa analysed, as did all chemical variables analysed (with nitrate, phosphate and silicate

in particular performing consistently well), oxygen variables (with apparent oxygen utilisation, in particular, scoring highly) and temperature. AUC values for hydrodynamic variables were generally low, but regional flow rate consistently outperformed vertical flow rate (Table 3). The highest scoring variables in each variable group for each taxon were chosen for use in the multivariate Maxent models (see Tables 3 and 4).

#### 3.3. Multivariate model evaluation

Test AUC scores for the multivariate Maxent models were high (Table 4), ranging from 0.836 (Xenophyophorea) to 0.997 (*S. fragilissima*). Test gain values ranged from 0.841 (Xenophyophorea) to 4.580 (*S. fragilissima*), while entropy values ranged from 8.632 (Xenophyophorea) to 4.512 (*S. fragilissima*). Test omission scores were low, ranging from 0.200 (Xenophyophorea) to 0.000 (*S. fragilissima* and *S. zonarium*) (based on the maximum sensitivity plus specificity of the test dataset). These low omission scores indicate that few known presences were wrongly classified as absences by the models, and that the predicted presences were significantly more probable than that of random background pixels (Table 4).

#### 3.4. Taxa niches

Jack-knife assessment of model regularised training gain was used to determine which three variables were most important in the production of each of the multivariate Maxent models (Table 4). Combining this with information presented in Fig. 2, the main environmental conditions for peak habitat suitability (defined as a logistic habitat suitability of  $\geq 0.5$ ) – i.e. the niche – for each taxon were estimated. For *S. fragilissima* these were a depth of between  $\sim 830$  and 1180 m, a calcite saturation state of between  $\sim 2.6$  and 3.4, and a temperature of between  $\sim 5.3$  and 7.7 °C. For *S. zonarium*, these were a nitrate concentration greater than  $37.5 \mu\text{mol l}^{-1}$ , apparent oxygen utilisation values between 4.5 and  $6.3 \text{ mol O}_2 \text{ m}^{-3}$ , and temperatures between 1.6 and 4.7 °C.

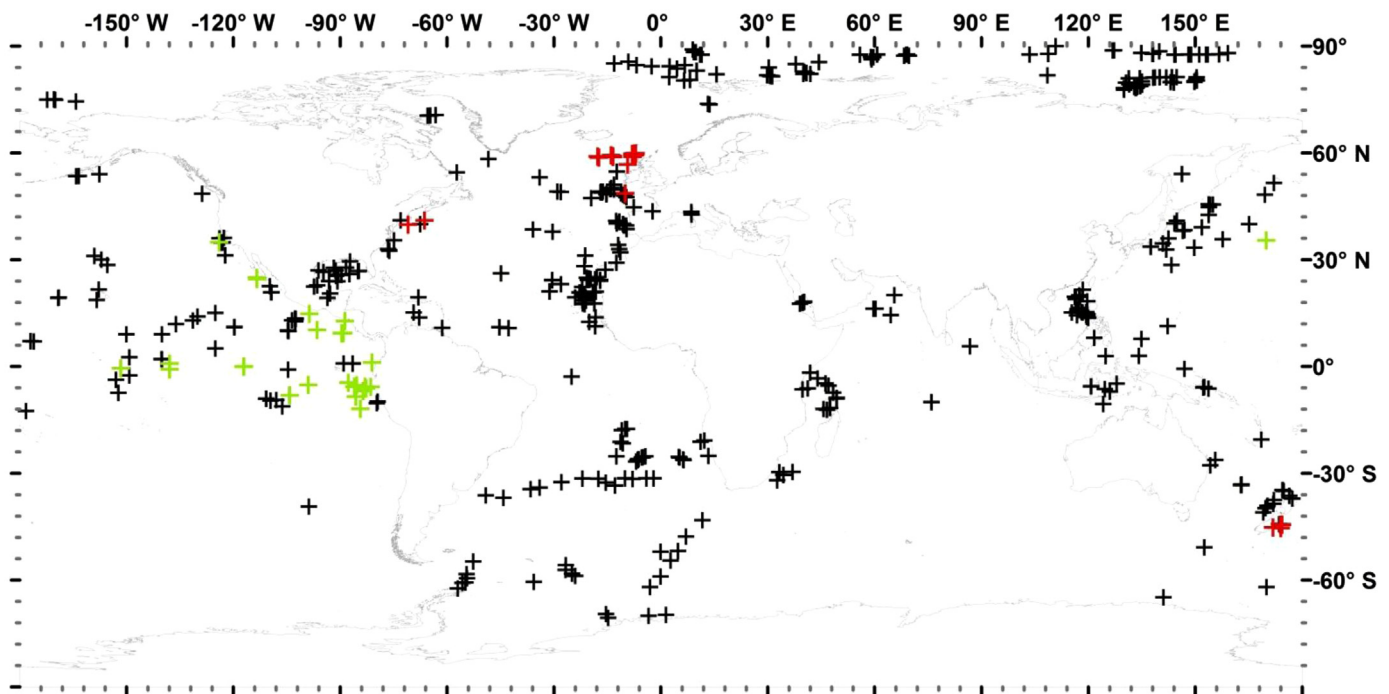
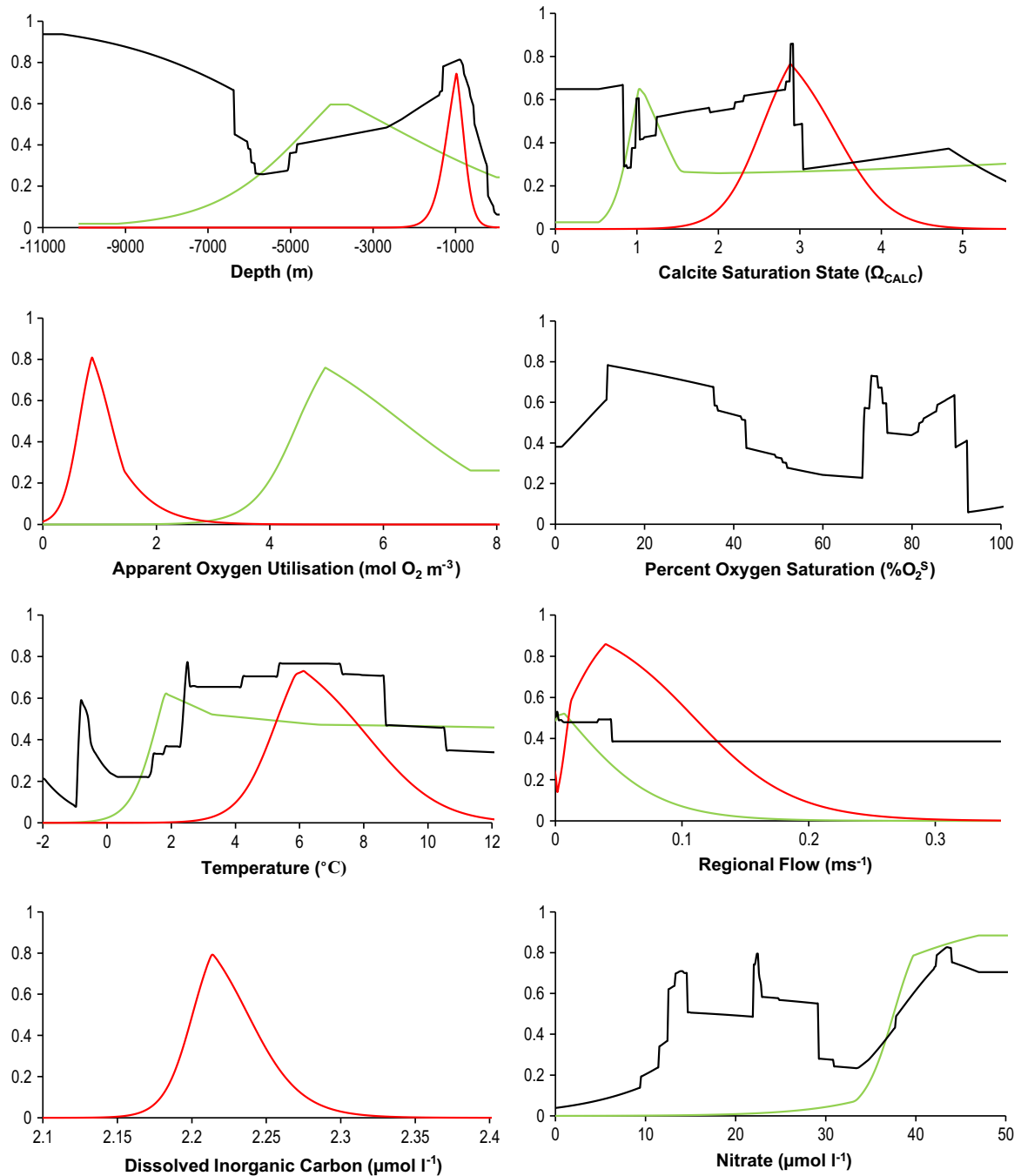


Fig. 1. Global sampling locations for xenophyophores. Taxa are colour-coded: *Syringammina fragilissima* – red; *Stannophyllum zonarium* – green; remaining Xenophyophorea – black. (For interpretation of the references to colour in this figure legend, the reader is referred to the web version of this article.)



**Fig. 2.** Variable response curves for global Maxent habitat suitability models of xenophyophore taxa. Note that Y axis is habitat suitability – 0 (min) to 1 (max) in all cases. Taxa are colour-coded as in Fig. 1: Xenophyophorea – black; *Syringammina fragilissima* – red; *Stannophyllum zonarium* – green. (For interpretation of the references to colour in this figure legend, the reader is referred to the web version of this article.)

It is more complex to estimate conditions of peak habitat suitability for Xenophyophorea since the model encompasses the varied habitat requirements of multiple species (including those described above) and hence produced variable responses that had multiple peaks (Fig. 2). Considering this, high habitat suitability for the taxon occurred at nitrate concentrations of  $\sim 12.5$  to  $29.2 \mu\text{mol l}^{-1}$  and above  $38.0 \mu\text{mol l}^{-1}$ , oxygen saturations between 6.6% and 42.6%  $\text{O}_2^s$ , between 69.2% and 74.3%  $\text{O}_2^s$  and between 82.1% and 90.0%  $\text{O}_2^s$ , and temperatures ranging from  $\sim -0.8$  to  $-0.6^{\circ}\text{C}$  and  $\sim 2.4$  to  $8.7^{\circ}\text{C}$ .

For Xenophyophorea and *S. fragilissima*, temperature was the variable that both reduced the training gain by the greatest

amount when omitted from the multivariate Maxent model and produced the highest gain when used in isolation. Hence, this variable contained the most useful information that was not present in the other variables used to construct the models and the most useful information when used in isolation (Table 4). For *S. zonarium*, apparent oxygen utilisation contained the most information that was not present in the other variables and the most useful information when used in isolation (Table 4).

At the other end of the spectrum, regional flow rate consistently contributed very little to the Maxent multivariate models, whilst depth and calcite saturation state contributed relatively little to the niche model of *S. zonarium* (Table 4).

### 3.5. Areas of maximal habitat suitability

For Xenophyophorea (see Fig. 3 and S1), areas of peak habitat suitability were centred on a range of bathymetric features, including continental slopes, subduction trenches, semi-enclosed seas, ridges, seamounts and plateaus. In the Atlantic, xenophyophore habitat suitability was high along all continental slopes, around the Rio Grande Rise, along the Walvis, Reykjanes and Mid-Atlantic Ridges, in the Gulf of Guinea, on the Cape Verde Plateau and plain, in the Angola, Porcupine and Biscaya abyssal plains, the most westerly extent of the Mediterranean Sea, around Rockall Bank and the Icelandic Plateau, along the Davies Strait and in Baffin Bay, around the Flemish Cap, in the Gulf of Mexico, and in deep water areas off Florida and in the Caribbean Sea. Habitat suitability was essentially zero on all continental shelves, in all but the very western extent of the Mediterranean and Sargasso seas, on the Sohm and Hatteras Plains, and in the, Sierra Leone, Guinea, Brazil, Argentine and Cape Verde Basins.

Habitat suitability was moderate in the Arctic Ocean (between 0.3 and 0.8 logistic suitability), and hotspots were centred upon the continental slopes, Voring Plateau, Greenland Sea, Denmark Strait, Baffin Bay, and Lomonosov Ridge (Fig. 3).

The Southern and Indian Oceans exhibited only isolated areas of high habitat suitability for xenophyophores, relative to the Atlantic Ocean. These included points along continental slopes (save for the Antarctic continental slope), the South Tasman Rise and the Exmouth Plateau, along Broken Ridge, scattered points along Ninetyeast Ridge, parts of the Agulhas, Madagascar and Mozambique plateaus, regions of the Carlsberg ridge, along the Chagos-Laccadive ridge, the Mascarene Plateau, and regions of high suitability in the north of the Bay of Bengal, the Lakshadweep Sea, Gulf of Aden and deepest parts of the Red Sea. Further south, the South Sandwich Trench is also notable for relatively high habitat suitability (Fig. 3).

The Malay Archipelago exhibited very high habitat suitability for xenophyophores in general. Particularly suitable areas included the Andaman Sea (particularly Drednought Bank) and the South China Sea, Sulu Sea, Celebes Sea and Banda Sea. In the southwest Pacific, the Bismarck Sea, Ontong Java Rise and regions of the Coral Sea showed areas of relatively high habitat suitability. Regions of suitable habitat were also found around New Zealand – particularly on the Challenger Plateau and Chatham Rise, and along the Kermadec and Tonga trenches and associated ridges (Fig. 3).

In the Pacific proper, high habitat suitability was generally centred along subduction trenches, continental slopes and numerous seamounts; for example, along the Mariana, Ryukyu, Izu-Ogasawara, Japan and Kuril-Kamchatka trenches and associated ridges to the west, the Mid-Pacific Mountains, Emperor Seamount chain, and around the Hawaiian ridge and Islands. High habitat suitability was also highlighted along the Cocos and Carnegie Ridges, along the length of the Peru-Chile Trench, in the deep water off the Californian coast, the northern-most extent of the Bering Sea, in the deeper regions of the Sea of Okhotsk and to the west of the Ryukyu Islands (Fig. 3).

The model for *S. fragilissima* produced the smallest area of suitable habitat of the taxa investigated (Table 4, Fig. 4 and S2), being restricted to around Rockall Bank, the Hebrides Terrace and Anton Dohrn Seamounts, Rosemary Bank, along the Wyville Thomson Ridge, points on the continental slope along the west of the United Kingdom, the Iceland-Faeroe Rise, the continental slope around Iceland and the Reykjanes Ridge, along the Mid-Atlantic Ridge close to the Azores, around the northernmost extent of the Labrador Sea, north of the Bahamas, along the shallowest regions of the Madagascar Plateau, and points around New Zealand (particularly in areas of the Campbell Plateau). Unfortunately, presence records for *S. fragilissima* are limited and also fairly well clustered, leading to the need to extrapolate over relatively large areas of the model, e.g. the South Atlantic, North

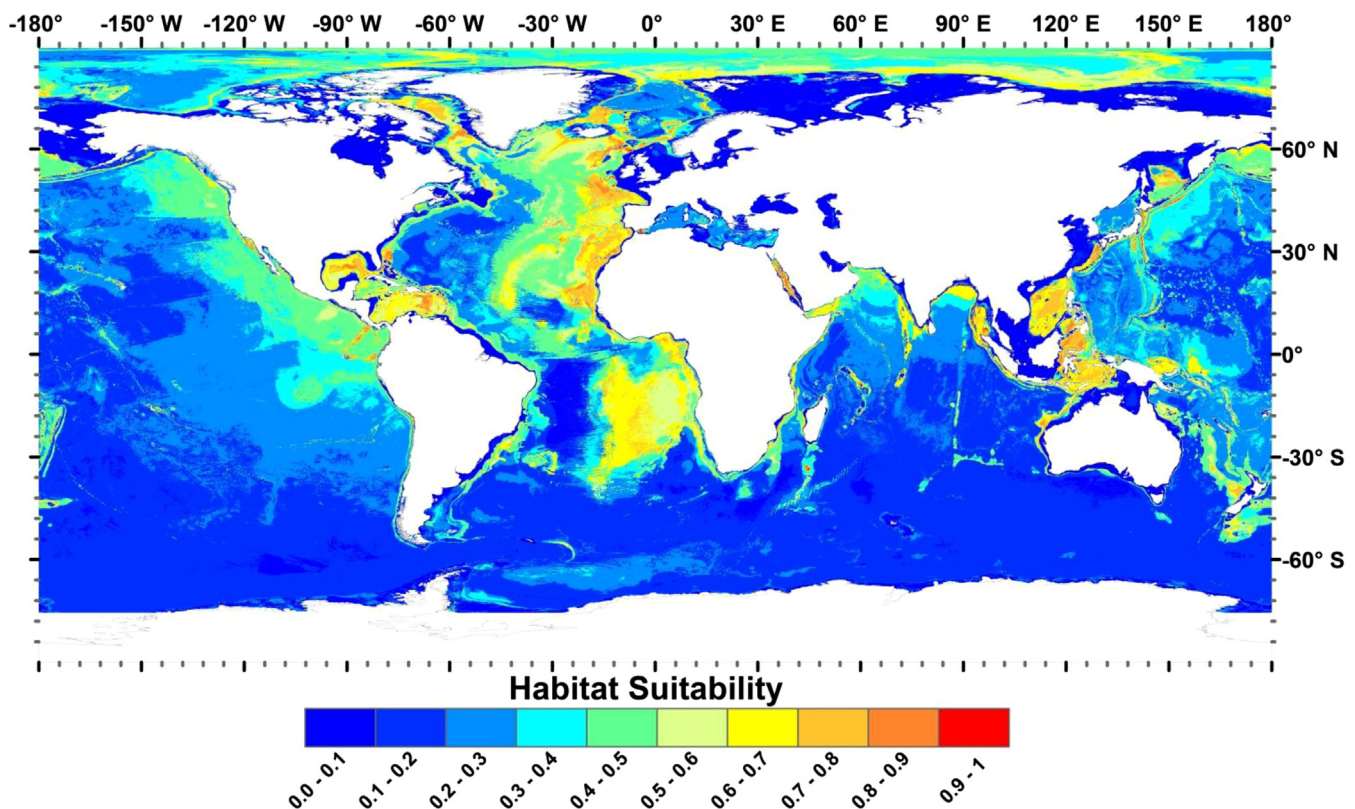
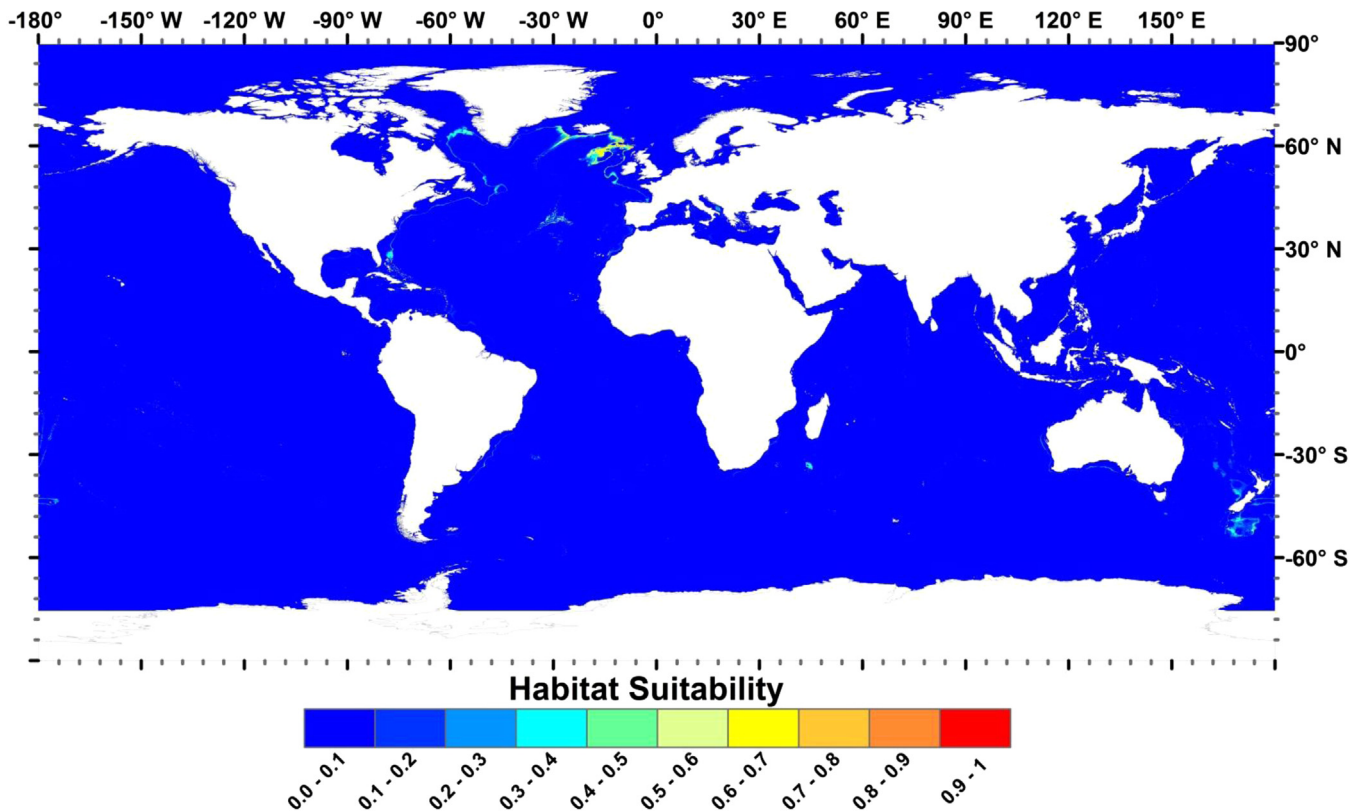


Fig. 3. Global habitat suitability for Xenophyophorea at 30' resolution. Based on Maxent output (logistic). Habitat suitability values of 0 illustrate minimally suitable environmental conditions in an area. Habitat suitability values of 1 illustrate maximally suitable environmental conditions in an area.





**Fig. 4.** Global habitat suitability for the xenophyophore species *Syringammina fragilissima* at 30' resolution. Based on Maxent output (logistic). Habitat suitability values of 0 illustrate minimally suitable environmental conditions in an area. Habitat suitability values of 1 illustrate maximally suitable environmental conditions in an area.

and East Pacific, Arctic and Indian Oceans. As a result, Fig. 4 may not represent the entire distribution of this species. The addition of further presence records (particularly in regions yet to be sampled) may alter the area of apparent high habitat suitability for *S. fragilissima*.

The model for *S. zonarium* (Figs. 5 and S3) highlights a broader distribution than for *S. fragilissima*, with areas of maximal habitat suitability centred on the Pacific Ocean rather than the Atlantic Ocean. Areas of high habitat suitability include much of the East and Northeast Pacific (Guatemala Basin and Albatross Plateau in particular), along the northern slope of the Aleutian Trench, around the Hawaiian Islands and Ridge, the Mid-Pacific Seamounts, along Sculpin Ridge, in the Aleutian Basin (particularly the northernmost extent), along the Emperor Seamount Chain, on the Hess and Shatsky rises, in the Kuril Basin, along the Mariana, Ryukyu, Izu-Ogasawara, Japan and Kuril-Kamchatka trenches and associated ridges to the west, to the south of Japan, the Ontong Java Rise, Caroline Seamounts, and isolated areas in the Coral Sea. In the Malay Archipelago, areas of high habitat suitability include deep areas of the Andaman, Sulu and South China seas, the Celebes Sea, the Makassar Strait and North Banda Basin, and areas of the Molucca and Flores Sea. In the Indian Ocean, the northernmost extent of the Bay of Bengal, regions of the Arabian Sea and Gulf of Aden, points along the Mascarene and Chagos-Laccadive plateaus and areas of continental slope along the northern shores of the ocean show high habitat suitability for this species (Fig. 5). However, as for *S. fragilissima*, this distribution should not be interpreted as definitive due to the relatively small number of presence records available and the need to extrapolate the model over such areas as the Indian, Atlantic and polar oceans. The addition of further presence records may alter the area of apparent high habitat suitability for *S. zonarium*.

## 4. Discussion

### 4.1. Habitat predictions and applications

This exploratory study enhances both our knowledge of xenophyophore distributions and illuminates the controlling physical factors of these distributions. It is generally accepted that xenophyophores reach highest densities in regions of high surface productivity (Tendal, 1972), and in areas where the flux of organic particles is enhanced by topography (Levin and Thomas, 1988; Levin, 1994; Gooday et al., 2011), including seamounts, mid-ocean ridges, canyons, subduction trenches, plateaus and continental slopes (Lemche et al., 1976; Tendal and Lewis, 1978; Levin and Thomas, 1988; Levin, 1994; Gooday et al., 2011). These topographic features are associated with localised currents (e.g. Roden, 1987), and thus it is hypothesised that organic particles are concentrated in their vicinity, increasing food availability for xenophyophores. As an alternative, Levin and Thomas (1988) suggest that the localised current regimes around these topographic features result in an increased flux and/or deposition of xenophyophore propagules. Predicted xenophyophore distributions (Figs. 3–5) were broadly concordant with the accepted views outlined above despite the fact that productivity or localised current flow data were not available for use in this analysis (although apparent oxygen utilisation can be thought of as a proxy for productivity, and terrain variables can capture topographically-driven flow patterns). High habitat suitability values were commonly obtained for mid-ocean ridges, continental slopes, plateaus, seamounts and the slopes of subduction trenches. This suggests that these topographic features may be associated with additional environmental characteristics positive to xenophyophore growth. Interestingly, in addition to the topographic features outlined above, this analysis

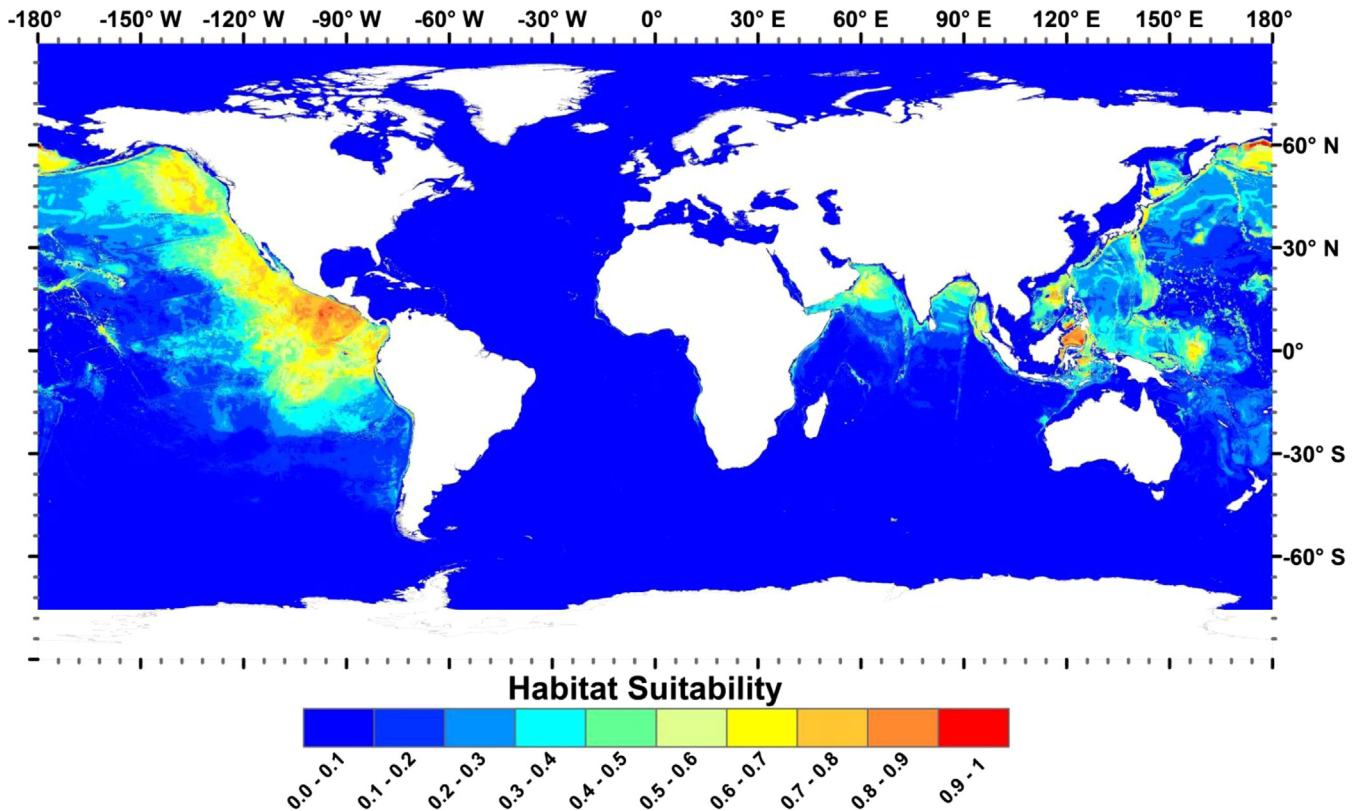


Fig. 5. Global habitat suitability for the xenophyophore species *Stannophyllum zonarium* at 30' resolution. Based on Maxent output (logistic). Habitat suitability values of 0 illustrate minimally suitable environmental conditions in an area. Habitat suitability values of 1 illustrate maximally suitable environmental conditions in an area.

suggests that deep semi-enclosed seas and bays may also be favourable to xenophyophore growth. For example, Baffin Bay, the Gulf of Mexico, the Caribbean Sea, the South China Sea, Andaman Sea, Sulu Sea, Celebes Sea and Banda Sea all exhibit high habitat suitability (Fig. 3), although the Mediterranean Sea is an exception.

Comparison of the global sampling distribution (Fig. 1) and the habitat suitability map for xenophyophores (Fig. 3) reveals that some xenophyophores have been sampled from areas with relatively low predicted habitat suitability. These include the Mediterranean Sea, the Southern Ocean and along the coast of Antarctica, around the southernmost extent of the Brazil Basin and northernmost extent of the Argentine Basin, to the southeast of Sri Lanka, to the north of Madagascar and parts of the Northwest Pacific and Arctic Ocean. Incorrect identification or spatial referencing errors may explain some of these records. Alternatively, the xenophyophore distribution model may not fully reflect the potential distribution of the group, or these samples may represent collection of xenophyophores in fringe habitats where they naturally occur at low densities.

Comparison of xenophyophore sampling locations (Fig. 1) with the Maxent habitat suitability maps (Figs. 3–5) demonstrates that a significant number of locations with high predicted xenophyophore habitat suitability are yet to be sampled. For Xenophyophorea, these include much of the western Arctic Ocean, the Icelandic Plateau and Reykjanes Ridge, most of Baffin Bay and the Labrador Sea, around the Flemish Cap, much of the Caribbean Sea, the Angola Basin, many locations along the continental slopes of the East and West Atlantic, most of the Mid-Atlantic Ridge, the Madagascar and Mascarene plateaus, the Gulf of Aden, the north of the Bay of Bengal and much of the Indian Ocean continental slopes of Australia, the Andaman Sea and seas around Sulawesi in the Malay Archipelago, around the Ryukyu Islands, the Ontong Java

Rise, the northernmost extent of the Bearing Sea, much of the Sea of Okhotsk, and numerous seamounts in the Pacific Ocean. For *S. fragilissima*, such areas are less numerous, but include the Reykjanes Ridge and the Mid-Atlantic Ridge around the Azores, the northernmost extent of the Labrador Sea, and potentially to the north of the Bahamas and on Walters Shoal of the Madagascar Plateau. For *S. zonarium*, such areas are numerous and include much of the East and Northeast Pacific, along the Hawaiian and Boudeuse ridges, the deepest parts of the Bering Sea (particularly the northern slopes of the Aleutian Basin), along the Emperor Seamount Chain, along the major trenches of the West Pacific, on the Ontong Java Rise, the Andaman, South China, Sulu, Celebes and Banda Seas, the north of the Bay of Bengal, and the Arabian Sea. These locations represent key targets for future sampling.

Where they are abundant, large, morphologically complex but fragile xenophyophore species represent important ecosystem engineers, playing a significant role in biological processes at the sediment-water interface (Tendal, 1972; Levin and Thomas, 1988; Levin, 1991; Levin and Gooday, 1992; Smith et al., 2003; Hughes and Gooday, 2004; Hori et al., 2013). Dense populations of these protists would therefore support the establishment of MPAs in regions where human activities threaten deep-sea benthic environments. The present study may help to guide this process by identifying areas of high predicted xenophyophore habitat suitability that are currently subject to deep-sea trawling. Such areas include a large number of seamounts, banks, ridges and plateaus across the world's oceans (Fig. 3) (e.g. Koslow et al., 2000; Thrush and Dayton, 2002). Indeed, some such areas, including the Darwin Mounds off the NW coast of Scotland (De Santo and Jones, 2007), have already been protected based on the presence of vulnerable marine ecosystems, including xenophyophore aggregations. This analysis could also provide spatial guidance for the protection of areas vulnerable to local ecosystem impacts associated with

deep-sea oil and gas drilling, for example, around the 'Atlantic Frontier' drilling sites near the Faroe Islands, and in the Gulf of Mexico (Glover and Smith, 2003) (Fig. 3). Similar applications are possible in areas earmarked for deep-sea mining operations, notably parts of the Manus Basin off New Guinea and the Havre Trough off New Zealand (Glover and Smith, 2003), as well as the Clarion-Clipperton Fracture zone in the Eastern Pacific, where xenophyophores are known to reach quite high abundances (Kamenskaya et al., 2013) (Figs. 3 and 5). However, it should be stressed that, although the resolution of this analysis is very high at a global scale, it is not adequate for probing the fine-scale distributions of xenophyophores within areas of high apparent habitat suitability. Targeted surveys and distribution modelling of potential MPA locations at local or regional scales should be undertaken to ensure that protected areas are based on the highest quality observational data available (Rengstorf et al., 2012; Ross and Howell, 2012; Guinotte and Davies, 2012; Rengstorf et al., 2013).

#### 4.2. Taxa niches

Depth was one of the most important variables defining habitat suitability for the taxa analysed (Table 4). Moving from sea-level to greater depths, habitat suitability increased to values over 0.5 only in depths greater than about 500 m (Fig. 2). This agrees well with the accepted observation that xenophyophores are found in water depths greater than ~500 m (Tendal, 1972; Levin, 1994; Buhl-Mortensen et al., 2010). The importance of depth was not unexpected since multiple factors of biological importance also change with depth, including light intensity, pressure, temperature, productivity, salinity, calcium carbonate saturation states, and many more chemical variables. The trough in xenophyophore habitat suitability between about 4800 and 6350 m depth was unexpected, however (Fig. 2). It is possible that this is caused by unfavourable environmental conditions for xenophyophores at these depths, such as nutrient-depletion. Alternatively this trough could reflect the lack of environmental data available at depths of > 5500 m from many global data products (i.e. World Ocean Atlas). What is most likely, however, is that this habitat suitability trough represents an artefact of poor sampling effort at these depths.

Nitrate concentration was found to be an important environmental parameter for both Xenophyophorea as a whole and for *S. zonarium*. Peak habitat suitability occurred in waters with relatively high nitrate concentrations in the case of Xenophyophorea, and at particularly high nitrate concentrations (maximal at > 37.5  $\mu\text{mol l}^{-1}$ ) for *S. zonarium* (Fig. 2). This finding agrees well with the observation that xenophyophores are most common in relatively nutrient-enriched waters (Tendal, 1972; Levin and Thomas, 1988; Levin, 1994; Gooday et al., 2011).

As far as we are aware, the importance of the calcite saturation state as a habitat characteristic relevant to xenophyophore distributions (Table 4) has never been explicitly stated. However, xenophyophores often exhibit a 'preference' for sand-sized particles in test construction (Levin and Thomas, 1988; Levin, 1994), and planktonic foraminiferal shells are a common sand-sized test component in many cases (A. Gooday, personal communication). It seems that for many (but certainly not all) xenophyophore species, a calcite saturation state > 1 is associated with test production from recycled calcareous foraminifera. For example, *S. fragilissima*, a species that incorporates numerous foraminiferal shells into its test (Tendal, 1972), occurs well above the carbonate compensation depth and experiences peak habitat suitability in waters with a calcite saturation state of between ~2.56 and 3.36 (Fig. 2).

Oxygen variables were important in model construction for Xenophyophorea and for *S. zonarium* in this study. Per cent oxygen saturation was an important variable for Xenophyophorea (Table 4), which exhibited peaks of habitat suitability at saturations ranging

from 7 up to 90% $\text{O}_2^{\text{S}}$  (Fig. 2). Such a broad range of suitable oxygen saturations demonstrates a high level of variability in oxygen requirements and tolerance amongst species in this taxon, although most xenophyophores have been sampled from relatively well-oxygenated regions (A. Gooday, personal communication). Apparent oxygen utilisation was the most important variable in the construction of the Maxent model for *S. zonarium*. Interestingly, this species reaches peak densities at apparent oxygen utilisation values of between 4.50 and 6.32  $\text{mol O}_2 \text{m}^{-3}$  (Fig. 2). Such high values link well with the high nitrate concentration preferences of *S. zonarium*, suggesting that this species is often sampled from productive nutrient enriched regions with particularly high associated biological activity.

Temperature was of consistent importance to all taxa investigated, and was the single most important variable in the construction of the Maxent models for Xenophyophorea and *S. fragilissima* (Table 4). The two species investigated in detail exhibited discrete temperature windows of peak habitat suitability (between ~5.3 and 7.7 °C for *S. fragilissima*, compared to between ~1.6 and 4.7 °C for *S. zonarium*) (Fig. 2). The relationship between the occurrence of xenophyophores and temperature is not well understood. This topic is briefly discussed by Tendal (1972) who argues that, as xenophyophores are members of a distinct cold-water fauna, their upper depth limits are constrained by temperature, although he does not consider why this should be. Such relationships are well documented for marine invertebrates generally (e.g. Orton, 1920; Carney, 2005; Barras et al., 2009), with temperature being an important factor controlling growth rate and various aspects of reproductive physiology, mediated by its influence on biochemical reactions (Brown et al., 2004).

Finally, it is interesting to note the low AUC values (Table 3) and low jack-knife training gains (Table 4) that were obtained for the hydrodynamic variables for all taxa investigated (regional flow for *S. fragilissima* being a potential exception). This was surprising since the importance of water flow for xenophyophores, some of which are likely to be suspension feeders, has been stressed by many authors (Tendal, 1972; Tendal and Lewis, 1978; Levin and Thomas, 1988; Levin, 1994). However, hydrodynamic variables also performed badly in a recent study, using a similar environmental dataset, of the distributions of cold-water corals, which are known suspension feeders (Yesson et al., 2012). Thus this poor performance is likely to represent a scale issue; i.e. these global scale layers not accurately portraying local scale variations in current velocity associated with small topographic features (Yesson et al., 2012). Higher resolution data is required to shed further light on the importance of current flow for the distribution of megafaunal suspension-feeders (Mohn et al., 2014).

#### 4.3. Model evaluation and limitations

Model performance was good for all taxa, with high test AUC and gain scores, and low test omission values. Test AUC and gain values were higher for the species investigated compared to xenophyophores as a whole, and were higher for *S. fragilissima* than for *S. zonarium*. This was probably a result of the greater level of clustering of *S. fragilissima* sample locations relative to *S. zonarium*. The models for *S. fragilissima* and *S. zonarium* had a less variable dataset to fit than for Xenophyophorea, with smaller total variance in the environmental parameters at their sampling localities (smaller entropy values – see Table 4) as a result of the smaller number of presence records used in the models. Thus the Maxent model could be fitted more tightly around the presence data.

There are known issues associated with species distribution models produced using small numbers of presence records (Feely and Silman, 2011), these chiefly being over-prediction resulting in false positives (Anderson and Gonzalez, 2011), and false negatives.



The use of presence records that are distributed across a large longitudinal and latitudinal range (as for the model for Xenophyophorea) should lower the risk of over-prediction, and in general, the models appear to have performed well. However, there is some evidence of small areas of false positives. For example, in Fig. 3 (Xenophyophorea), relatively shallow areas (< 500 m depth) of the Norwegian trough are highlighted as potentially suitable habitat (0.4–0.6 logistic habitat suitability), while in Fig. 5 (*S. zonarium*), small areas of the Shelikof Strait are highlighted as suitable habitat (0.7–0.9 logistic habitat suitability) in water depths of around 200 m. Considering our current knowledge of xenophyophore bathymetric distributions (see above and Fig. 2), these predictions almost certainly represent false positives, although only ground-truthing can confirm this. False negatives are harder to pinpoint in the Maxent predictions, but very probably occur to some extent in the models for *S. fragilissima* and *S. zonarium* (considering the level of extrapolation across ocean basins from a relatively small number of presence records). The addition of further presence records (particularly in regions yet to be sampled) will help to better define the distributions of these two species and highlight any false negatives present in the current models.

Comparison of the habitat suitability predictions obtained in the present study with those of the only other Maxent model yet produced for a xenophyophore species (Ross and Howell, 2012) represents a further way in which model performance can be evaluated. In general, the two models show a high level of similarity. High habitat suitability (> 0.6) for *S. fragilissima* in the NE Atlantic is demonstrated in both models along the continental slope off Ireland and the United Kingdom, around the Hebrides Terrace and Anton Dohrn seamounts, around Rosemary Bank, and along the slopes of Rockall and Hatton banks. There are some areas where the two models disagree, however. For instance, the model of Ross and Howell predicts higher *S. fragilissima* habitat suitability around the slopes of Edoras and Fangorn banks and along the slopes of the Porcupine Seabight and Goban Spur relative to the model presented in this paper. In addition, our model predicts larger areas of high habitat suitability, relative to Ross and Howell (2012), for *S. fragilissima* to the south of the Wyville-Thomson Ridge, between Bill Bailey's Bank and Rosemary Bank, and in the Hatton-Rockall Basin. The overall similarity of the two models, however, gives further confidence to their predictions, especially considering that they are produced from different data sets – Ross and Howell choosing only to use topographic data.

Choice of modelling resolution is an important factor when producing predictive species distribution models (Guisan et al., 2007). While higher resolution outputs are preferable when we need to capture environmental variability at small spatial scales (like the rapid changes in temperature that occur with distance across the Faroe-Shetland Channel (Oey, 1997)) and for visualising predictions, they do involve certain associated errors and limitations (Davies et al., 2008; Davies and Guinotte, 2011). Apart from depth, global environmental layers are not available at 30' resolution, and so variables have to be up-scaled from their native resolution to that required (30' in this analysis – see Methods). Up-scaling inevitably introduces some error, which grows as the difference between native and required resolution increases (Davies and Guinotte, 2011). This leads, for example, to the generalisation and smoothing of variables and the failure to capture some aspects of small scale variability (since this information is not present in the lower resolution source data) (Davies and Guinotte, 2011; Rengstorf et al., 2012). Further, the majority of global layers currently available that can be up-scaled represent annual means of values (in order to ensure a high number of samples to maximise certainty in the variables (Davies and Guinotte, 2011)). As a result, these layers do not capture any component of annual variability, a particular drawback when modelling highly seasonal high latitude regions.

However, comparison of up-scaled data with GLODAP (Global Ocean Data Analysis Project) test bottle water data by Davies and Guinotte (2011) found the two datasets to be highly correlated, and hence the authors concluded that any issues associated with the up-scaling method are outweighed by its benefits.

Whilst the dataset utilised in this study comprised a high number and diversity of variables, other variables that may have been informative were not available for use. Chief amongst these were productivity variables, such as measures of particulate organic carbon reaching the seafloor, and surface water chlorophyll a concentrations. These variables were not available owing to a rapid decline in data quality at latitudes greater than ~70° (see Section 2.2). Substratum type is a further variable that would have been interesting to incorporate into this analysis as there is evidence for sediment-type preference in xenophyophores (Levin and Thomas, 1988). Unfortunately, a global environmental layer containing details of sediment type is not yet available, although progress is being made towards this goal (e.g. Shumchenia and King, 2010). Furthermore, the hydrodynamic variables used in this study under-performed and were not of sufficient sensitivity to capture local scale variation in flow rates associated with isolated topographic features such as seamounts. Thus, considering the current uncertainty surrounding xenophyophore feeding methods, it would be particularly interesting to incorporate a high resolution local current flow into future analyses. Such a layer is currently unavailable at a global scale, although advances are being made at the regional scale (Mohn et al. 2014).

Potential evidence for xenophyophore sampling bias has been mentioned in Section 3.1. Firm evidence of sampling bias would imply that the current distribution of presence localities used in this study is not adequate to represent all potential environments from which xenophyophores can be sampled. This would potentially lead to false negatives in the Maxent outputs. Whether this is the case will only become apparent following further sampling and analyses.

The most conclusive way to validate or refute the predictions of this analysis (Figs. 3–5) would be to directly test them in the field via 'ground-truthing' (Guinotte and Davies, 2012). Do we find xenophyophores in areas of predicted high habitat suitability that have not yet been suitably sampled, like the Andaman Sea, or do these predictions represent false positives? There are some issues with this method. Assuming that a cruise to undertake this task could be funded, it would be a huge undertaking to systematically search an entire 30' cell of high predicted habitat suitability using ROVs or camera equipment, and subsampling may miss specimens as xenophyophore distributions may be patchy within this cell. However, it should be noted that xenophyophores have been recorded at very high densities in areas of suitable habitat (Tendal and Gooday, 1981), increasing the likelihood of discovery.

A comparison of the results of Davies et al. (2008) with those of Davies and Guinotte (2011) and Yesson et al. (2012) demonstrates how rapidly species distribution modelling has progressed in recent years in terms of resolution. Model performance criteria have also improved significantly (e.g. Warren and Seifert, 2011). The availability of additional relevant environmental variables with global coverage at high resolution, and a growing number of reliable presence localities, will continue to lead to increasingly accurate models suitable for a number of research and industrial applications.

#### 4.4. Concluding remarks

This study represents the first of its kind for xenophyophores at a global scale and serves to improve knowledge of their distributions and further illuminate details of their ecology. Additionally, this analysis draws attention to the possible use of these fragile



and remarkable deep-sea megafaunal ecosystem engineers in enhancing MPA planning and designation. However, this work only represents a first step and aims to motivate continued research into the factors controlling the distribution of these intriguing and important organisms. Further advances will be achieved by testing model predictions with further sampling, performing local-scale high-resolution analyses, and addressing some of the still unanswered questions concerning xenophyophore ecology and physiology.

## Acknowledgements

The authors would like to thank Prof. Andrew Gooday for his frequent advice and insightful comments, which have much improved this manuscript, Dr. Ole Tendal for advice concerning the availability of records of xenophyophore sampling locations, especially for *Stannophyllum zonarium*, and three anonymous reviewers for their detailed recommendations. Dr. Daniel Jones was funded for this work by the UK National Environment Research Council as part of the Marine Environmental Mapping Programme (MAREMAP).

## Appendix A. Supporting information

Supplementary data associated with this article can be found in the online version at <http://dx.doi.org/10.1016/j.dsr.2014.07.012>.

## References

- Anderson, R.P., Gonzalez Jr., I., 2011. Species-specific tuning increases robustness to sampling bias in models of species distributions: an implementation with Maxent. *Ecol. Modell.* 222, 2796–2811.
- Barras, C., Geslin, E., Duplessy, J.-C., Jorissen, F.J., 2009. Reproduction and growth of the deep-sea benthic foraminifer *Bulimina marginata* under different laboratory conditions. *J. Foraminif. Res.* 39, 155–165.
- Beaumont, L.J., Hughes, L., Poulsen, M., 2005. Predicting species distributions: use of climatic parameters in BIOCLIM and its impact on predictions of species' current and future distributions. *Ecol. Modell.* 186, 251–270.
- Becker, J.J., Sandwell, D.T., Smith, W.H.F., Braud, J., Binder, B., Depner, J., Fabre, D., Factor, J., Ingalls, S., Kim, S.-H., Ladner, R., Marks, K., Nelson, S., Pharaoh, A., Trimmer, R., Von Rosenberg, J., Wallace, G., Weatherall, P., 2009. Global bathymetry and elevation data at 30 arc seconds resolution: SRTM30\_PLUS. *Mar. Geod.* 32, 355–371.
- Bisby, F.A., Roskov, Y.R., Orrell, T.M., Nicolson, D., Paglinawan, L.E., Bailly, N., Kirk, P. M., Bourgoin, T., Baillargeon, G., (Eds.), 2010. Species 2000 & ITIS Catalogue of Life: 2010 Annual Checklist Taxonomic Classification. DVD; Species 2000: Reading, UK.
- Boyer, T.P., Levitus, S., Garcia, H.E., Locarnini, R.A., Stephens, C., Antonov, J.I., 2005. Objective analyses of annual, seasonal, and monthly temperature and salinity for the World Ocean on a 0.25° grid. *Int. J. Climatol.* 25, 931–945.
- Brady, H.B., 1879. Notes on some of the Reticularian Rhizopoda of the "Challenger" expedition. Part 1. On new or little known arenaceous types. *Q. J. Microsc. Sci.* 19, 20–63.
- Brady, H.B., 1883. *Syringammina*, a new type of arenaceous Rhizopoda. *Proc. R. Soc.* 35, 55–161.
- Brady, H.B. 1884. Report on the Foraminifera. Report on the Scientific Results of the Voyage of H. M. S. Challenger, vol. 9, pp. 1–814.
- Brown, J.H., Gillooly, J.F., Allen, A.P., Savage, V.M., West, G.B., 2004. Toward a metabolic theory of ecology. *Ecology* 85 (7), 1771–1789.
- Buhl-Mortensen, L., Vanreusel, A., Gooday, A.J., Levin, L.A., Priede, I.G., Buhl-Mortensen, P., Gheerardyn, H., King, N.J., Raes, M., 2010. Biological structures as a source of habitat heterogeneity and biodiversity on the deep ocean margins. *Mar. Ecol.* 31, 21–50.
- Carney, R.S., 2005. Zonation of deep biota on continental margins. *Oceanogr. Mar. Biol.: Annu. Rev.* 43, 211–278.
- Carton, J.A., Giese, B.S., Grodsky, S.A., 2005. Sea level rise and the warming of the oceans in the SODA ocean reanalysis. *J. Geophys. Res.* 110, C09006.
- Davies, A.J., Guinotte, J.M., 2011. Global habitat suitability for framework-forming cold-water corals. *PLoS ONE* 6, e18483.
- Davies, A.J., Wisshak, M., Orr, J.C., Roberts, J.M., 2008. Predicting suitable habitat for the cold-water reef framework-forming coral *Lophelia pertusa* (Scleractinia). *Deep Sea Res. Part I: Oceanogr. Res. Papers* 55, 1048–1062.
- De Santo, E.M., Jones, P.J.S., 2007. The Darwin Mounds: from undiscovered coral to the development of an offshore marine protected area regime. *Bull. Mar. Sci.* 81, 147–156.
- Elith, J., Graham, C.H., Anderson, R.P., Dudik, M., Ferrier, S., Guisan, A., Hijmans, R.J., Huettmann, F., Leathwick, J.R., Lehmann, A., Li, J., Lohmann, L.G., Loiselle, B.A., Manion, G., Moritz, C., Nakamura, M., Nakazawa, Y., McC. Overton, J., Peterson, A.T., Phillips, S.J., Richardson, K., Scachetti-Pereira, R., Schapire, R.E., Soberon, J., Williams, S., Wisz, M.S., Zimmernann, N.E., 2006. Novel methods improve prediction of species' distributions from occurrence data. *Ecography* 29, 129–151.
- Elith, J., Phillips, S.J., Hastie, T., Dudik, M., En Chee, Y., Yates, C.J., 2011. A statistical explanation of MaxEnt for ecologists. *Divers. Distrib.* 17, 43–57.
- Feeley, K.J., Silman, M.R., 2011. Keep collecting: accurate species distribution modelling requires more collections than previously thought. *Divers. Distrib.* 17, 1132–1140.
- Fielding, A.H., Bell, J.F., 1997. A review of methods for the assessment of prediction errors in conservation presence/absence models. *Environ. Conserv.* 24, 38–49.
- Garcia, H.E., Locarnini, R.A., Boyer, T.P., Antonov, J.I., 2006a. World ocean atlas 2005, volume 3: dissolved oxygen, apparent oxygen utilization, and oxygen saturation. In: Levitus, S. (Ed.), NOAA Atlas NESDIS 63. U.S. Government Printing Office, Washington, D.C., p. 342.
- Garcia, H.E., Locarnini, R.A., Boyer, T.P., Antonov, J.I., 2006b. World ocean atlas 2005, volume 4: nutrients (phosphate, nitrate, silicate). In: Levitus, S. (Ed.), NOAA Atlas NESDIS 64. U.S. Government Printing Office, Washington, D.C., p. 396.
- Glover, A.G., Smith, C.R., 2003. The deep-sea floor ecosystem: current status and prospects of anthropogenic change by the year 2025. *Environ. Conserv.* 30, 219–241.
- Gooday, A.J., Aranda da Silva, A., Pawlowski, J., 2011. Xenophyophores (Rhizaria, Foraminifera) from the Nazare Canyon (Portuguese margin, NE Atlantic). *Deep-Sea Res. II* 58, 2401–2419.
- Gooday, A.J., Bett, B.J., Pratt, D.N., 1993. Direct observation of episodic growth in an abyssal xenophyophore (Protista). *Deep-Sea Res.* 1 40, 2131–2143.
- Gooday, A.J., Tendal, O.S., 2002. Class Xenophyophorea. In: Lee, J.J., Huttner, J., Bovee, E.C. (Eds.), *An Illustrated Guide to the Protozoa*, 2nd ed. Society of Protozoologists and Allen Press, Lawrence, Kansas, pp. 1086–1097.
- Guinotte, J.M., Davies, A.J., 2012. Predicted Deep-sea Coral Habitat Suitability for the U.S. West Coast. Report to NOAA-NMFS. 85 pp.
- Guisan, A., Graham, C.H., Elith, J., Huettmann, F., 2007. Sensitivity of predictive species distribution models to change in grain size. *Divers. Distrib.* 13, 332–340.
- Haackel, E., 1889. Report on the deep-sea keratosa. Report on the scientific results of the voyage of H. M. S. Challenger during the years 1873–76. *Zoology* 32, 1–92.
- Hori, S., Tsuchiya, M., Nishi, S., Arai, W., Yoshida, T., Takami, H., 2013. Active bacterial flora surrounding Foraminifera (Xenophyophorea) living on the deep-sea floor. *Biosci., Biotechnol. Biochem.* 77, 381–384.
- Hughes, J.A., Gooday, A.J., 2004. Associations between living benthic foraminifera and dead tests of *Syringammina fragilissima* (Xenophyophorea) in the Darwin Mounds region (NE Atlantic). *Deep-Sea Res.* 1 51, 1741–1758.
- Jenness, J., 2012. DEM Surface Tools. Jenness Enterprises.
- Jones, K.H., 1998. A comparison of algorithms used to compute hill slope as a property of the DEM. *Comput. Geosci.* 24, 315–323.
- Kamenskaya, O.E., Melnik, V.F., Gooday, A.J., 2013. Giant protists (xenophyophores and komokiaceans) from the Clarion-Clipperton ferromanganese nodule field (Eastern Pacific). *Biol. Bull. Rev.* 3, 388–389.
- Koslow, J.A., Boehlert, G.W., Gordon, J.D.M., Haedrich, R.L., Lorange, P., Parin, N., 2000. Continental slope and deep-sea fisheries: implications for a fragile ecosystem. *J. Mar. Sci.* 57, 548–557.
- Laureillard, J., Mejanelle, L., Sibuet, M., 2004. Use of lipids to study the trophic ecology of deep-sea xenophyophores. *Mar. Ecol. Prog. Ser.* 270, 129–140.
- Lecroq, B., Gooday, A.J., Tsuchiya, M., Pawlowski, J., 2009. A new genus of xenophyophores (Foraminifera) from Japan Trench: morphological description, molecular phylogeny and elemental analysis. *Zool. J. Linn. Soc.* 156, 455–464.
- Lemche, H., Hansen, B., Madsen, F.J., Tendal, O.S., Wolff, T., 1976. Hadal life as analysed from photographs. *Vidensk Meddr Dansk Naturh Foren* 139, 263–336.
- Levin, L.A., 1991. Interactions between metazoans and large, agglutinating protozoans: implications for the community structure of deep-sea benthos. *Am. Zool.* 31, 886–900.
- Levin, L.A., 1994. Paleocology and ecology of xenophyophores. *Palaios* 9, 32–41.
- Levin, L.A., Gooday, A.J., 1992. Possible roles for xenophyophores in deep-sea carbon cycling. In: Rowe, G.T., Pariente, V. (Eds.), *Deep-sea Food Chains and the Global Carbon Cycle*. Springer, Netherlands, pp. 93–104.
- Levin, L.A., Thomas, C.L., 1988. The ecology of xenophyophores (Protista) on eastern Pacific seamounts. *Deep Sea Res.* 35, 2003–2027.
- Levin, L.A., DeMaster, D.J., McCann, L.D., Thomas, C.L., 1986. Effects of giant protozoans (class: Xenophyophorea) on deep-seamount benthos. *Mar. Ecol. – Prog. Ser.* 29, 99–104.
- Mohn, C., Rengstorf, A., White, M., Duineveld, G., Mienis, F., Soetaert, K., Grehan, A., 2014. Linking benthic hydrodynamics and cold-water coral occurrences: high-resolution model study at three cold-water coral provinces in the NE Atlantic. *Prog. Oceanogr.* 122, 92–104.
- Oey, L.-Y., 1997. Eddy energetic in the Faroe-Shetland channel: a model resolution study. *Cont. Shelf Res.* 17, 1929–1944.
- Ortega-Huerta, M.A., Peterson, A.T., 2008. Modelling ecological niches and predicting geographic distributions: a test of six presence-only methods. *Rev. Mex. Biodivers.* 79, 205–216.
- Orton, J.H., 1920. Sea-temperature, breeding and distribution in marine animals. *J. Mar. Biol. Assoc. U.K.* 12, 339–366.
- Pawlowski, J., Holzmann, M., Fahrni, J., Richardson, S.L., 2003. Small subunit ribosomal DNA suggests that the xenophyophorean *Syringammina corbicula* is a Foraminiferan. *J. Eukaryot. Microbiol.* 50, 483–487.

- Pfannkuche, O., 1993. Benthic response to the sedimentation of particulate organic matter at the BIOTRANS station, 47°N, 20°W. *Deep-Sea Res. II* 40, 135–149.
- Phillips, S.J., Anderson, R.P., Schapire, R.E., 2006. Maximum entropy modelling of species geographic distributions. *Ecol. Modell.* 190, 231–259.
- Phillips, S.J., Dudik, M., 2008. Modelling of species distributions with Maxent: new extensions and a comprehensive evaluation. *Ecography* 31, 161–175.
- Rengstorf, A.M., Grehan, A., Yesson, C., Brown, C., 2012. Towards high-resolution habitat suitability modelling of vulnerable marine ecosystems in the deep-sea: resolving terrain attribute dependencies. *Mar. Geod.* 35, 343–361.
- Rengstorf, A.M., Yesson, C., Brown, C., Grehan, A.J., 2013. High-resolution habitat suitability modelling of vulnerable marine ecosystems in the deep sea. *J. Biogeogr.* 40, 1702–1714.
- Richardson, S.L., 2001. *Syringammina corbicula* sp. nov. (Xenophyophorea) from the Cape Verde Plateau, E. Atlantic. *J. Foraminifer. Res.* 31, 201–209.
- Riemann, F., Tendal, O.S., Gingele, F.X., 1993. *Reticulammina Antarctica* nov. spec. (Xenophyophora, Protista) from the Weddell Sea, and aspects of the nutrition of xenophyophores. *Polar Biol.* 13, 543–547.
- Roden, G.L., 1987. Effects of seamounts and seamount chains on ocean circulation and thermohaline structure. In: Keating, B., Fryer, P., Batizar, R., Boehlert, G. (Eds.), *Seamounts, Islands, and Atolls*. Geophysical Monograph No. 43. American Geophysical Union, Washington D.C., USA, pp. 335–354.
- Ross, R.E., Howell, K.L., 2012. Use of predictive habitat modelling to assess the distribution and extent of the current protection of 'listed' deep-sea habitats. *Divers. Distrib.* 19, 433–445.
- Schulze, F.E., 1904. Über den Bau und die Entwicklung gewisser Tiefseeorganismen. *Sitzungsberichte der Königlich-preussischen Akademie der Wissenschaften zu Berlin*, 53, 1387.
- Schulze, F.E., 1907. Die Xenophyophoren: Eine besondere Gruppe der Rhizopoden. *Wissenschaftliche Ergebnisse der Deutschen Tiefsee-Expedition auf dem Dampfer "Valdivia" 1898–1899*. G. Fischer.
- Shumchenia, E.J., King, J.W., 2010. Comparison of methods for integrating biological and physical data for marine habitat mapping and classification. *Cont. Shelf Res.* 30, 1717–1729.
- Smith, C.R., Demopoulos, A.W.J., 2003. The deep Pacific ocean floor. In: Tyler, P.A. (Ed.), *Ecosystems of the Deep Oceans*. *Ecosystems of the World*, 28. Elsevier, Amsterdam, pp. 179–218. In: Tyler, P.A. (Ed.), *Ecosystems of the Deep Oceans*. *Ecosystems of the World*, 28. Elsevier, Amsterdam, pp. 179–218 (ISBN).
- Steinacher, M., Joos, F., Frolicher, T.L., Plattner, G.-K., Doney, S.C., 2009. Imminent ocean acidification in the Arctic projected with the NCAR global coupled carbon cycle-climate model. *Biogeosciences* 6, 515–533.
- Tendal, O.S., 1972. A Monograph of the Xenophyophoria (Rhizopodea, Protozoa) (Doctoral dissertation). Danish Science Press.
- Tendal, O.S., 1979. Aspects of the biology of Komokiacea and Xenophyophoria. *Sarsia* 64, 13–17.
- Tendal, O.S., 1996. Synoptic Checklist and Bibliography of the Xenophyophorea (Protista), with a Zoogeographical Survey of the Group. *Galathea Report* 17, (1995–1996), pp. 79–101.
- Tendal, O.S., Gooday, A.J., 1981. Xenophyophoria (Rhizopoda, Protozoa) in bottom photographs from the bathyal and abyssal NE Atlantic. *Oceanol. Acta* 4, 415–422.
- Tendal, O.S., Lewis, K.B., 1978. New Zealand xenophyophores: upper bathyal distribution, photographs of growth position, and a new species. *N. Z. J. Mar. Freshw. Res.* 12, 197–203.
- Thrush, S.F., Dayton, P.K., 2002. Disturbance to marine benthic habitats by trawling and dredging: implications for marine biodiversity. *Annu. Rev. Ecol. Syst.* 33, 449–473.
- Tittensor, D.P., Baco, A.R., Hall-Spencer, J.M., Orr, J.C., Rogers, A.D., 2010. Seamounts as refugia from ocean acidification for cold-water stony corals. *Mar. Ecol. Prog. Ser.* 31 (Suppl. 1), 212–225.
- Warren, D.L., Seifert, S.N., 2011. Ecological niche modelling in Maxent: the importance of model complexity and the performance of model selection criteria. *Ecol. Appl.* 21, 335–342.
- Wilson, M.F.J., O'Connell, B., Brown, C., Guinan, J.C., Grehan, A.J., 2007. Multiscale terrain analysis of multibeam bathymetry data for habitat mapping on the Continental Slope. *Mar. Geod.* 30, 3–35.
- Wisz, M.S., Hijmans, R.J., Li, J., Peterson, A.T., Graham, C.H., Guisan, A., 2008. NCEAS Predicting Species Distributions Working Group. 2008. Effects of sample size on the performance of species distribution models. *Divers. Distrib.* 14, 763–773.
- Yesson, C., Taylor, M.L., Tittensor, D.P., Davies, A.J., Guinotte, J., Baco, A., Black, J., Hall-Spencer, J.M., Rogers, A.D., 2012. Global habitat suitability of cold-water octocorals. *J. Biogeogr.* 39, 1278–1292.